Catalysis Letters 5 (1990) 113-126

A CATALYTIC AND CHARACTERIZATION STUDY OF THE SURFACE ACIDITY GENERATED ON THE REDUCTION OF COPPER EXCHANGED Y ZEOLITES

Brendan COUGHLAN and Mark A. KEANE *

Physical Chemistry Laboratories, University College, Galway, Eire

Received 1 October 1989; accepted 4 April 1990

Zeolite acidity, surface acidity, alkali metal co-cation, benzene ethylation, cumene cracking

Zeolite acidity, in the form of Bronsted acid sites generated on reducing a range of copper Y zeolites, was probed by infrared spectroscopy. The nature of the alkali metal co-cation (Li^+, Na^+, K^+, Rb^+ and Cs^+) is shown to influence both the acid strength and location of the Bronsted sites. Acid strength decreases in the order CuLiY > CuNaY > CuKY > CuRbNaY > CuCsNaY. The specific effect of the alkali metal co-stations on the level of protonic activity in benzene ethylation and cumene cracking is discussed.

1. Introduction

Zeolite acidity is represented by both Bronsted and Lewis acid sites. The former are protons attached to lattice oxygen atoms while the latter can be charge compensating cations or trigonal aluminium atoms at oxygen deficient sites or at cation sites. In the case of Bronsted acidity, it is generally accepted [1] that the lower the bond strength between the proton and the surface, the higher the acid strength of the proton. Hydroxyl groups located inside the supercages have been shown to be more acidic than those localized within the small cavities [2]. In general, the acidic properties are influenced by both the chemical environment of the framework oxygen atoms and by the intrinsic proton mobility; at a particular temperature the protons redistribute in the zeolite lattice so as to attain the minimum potential energy for the zeolite crystal. The electrostatic field of divalent transition metal cations is assumed to generate protons through a dissociation of the water of hydration. The stronger the electrostatic field of the cation, the greater the concentration of generated protons because of increased interaction of the cation with adsorbed water [3]. Migration of the cations within the zeolite framework results in changes in the surface field strength of the

---

* To whom correspondence should be addressed. Present address: Chemistry Department, The University, Glasgow, G12 8QQ, Scotland.

protonic sites [4]. Nevertheless, it has also been reported that heating a stoichiometrically Cu^{2+} exchanged Y zeolite did not result in the generation of any Bronsted acidity [6]. Hydrogen reduction of reducible transition metal cations also generates lattice hydroxyl groups according to [1,4,5]:

$$TM^{n+} + \tfrac{1}{2}H_2 \rightarrow TM^{(n-1)+} + 2H^+$$

which can be identified by infrared spectroscopy. Steinberg and co-workers observed that the concentrations of OH groups, generated on reduction of CuNaY, increased with increasing reduction temperature [7].

The study of correlations between the acidic and catalytic properties of acidic oxides has been a matter of interest for some time. The new field of zeolites has provoked an increase in the number of works related to this subject [1,8–27]. The alkylation of aromatics, in particular benzene and toluene, has been the subject of multilateral investigations over the past two decades [9–19], chiefly because of the importance of aromatic hydrocarbons in the petroleum industry. A fairly coherent understanding of the reaction mechanism has since evolved and it is now generally accepted that the alkylation process proceeds via a carbocation intermediate [9]. Both kinetic and mechanistic studies support a Rideal mechanism for alkylation with alcohols [9–11]. In the case of zeolites, it has been variously suggested that either Bronsted sites [12], Lewis sites [13] or the exchanged cations [14] are the loci of catalytic activity. Becker et al. [15] observed an optimum in the ethylation of benzene at an activation temperature of 723 K and concluded that Bronsted OH groups are the active sites; from a consideration of the product mixture, Yashima et al. [16] support this conclusion. In addition, Huang and Ko [19] have shown that the product, ethylbenzene, undergoes disproportionation and dealkylation to yield the starting material, benzene. Cumene dealkylation to benzene and propylene has also been used as a measure of the cracking activity of acid catalysis [20–25]. The reaction can be viewed as the reverse of an alkylation and is generally rationalized in terms of proton attack at an aromatic carbon atom with displacement of the side chain as a carbonium ion [1,20,21].

With a few exceptions [26,27], the majority of documented studies have been devoted to the characterization of NaHY zeolites with varying Na^+ content. In this paper, the acid function, generated on reduction in hydrogen of a wide range of monometallic copper exchanged Y zeolites enriched to various levels with different alkali metal cations is examined. Acid site generation is monitored by infrared spectroscopy and compared with that of a fully decationized HY zeolite. Benzene ethylation and cumene cracking are used as indices to probe the acidic catalytic activity of the reduced zeolites.

2. Materials and methods

The starting or parent zeolite was Linde Molecular Sieve LZY-52 (formula: $Na_{58}(AlO_2)_{58}(SiO_2)_{134}(H_2O)_{260}$). The samples under examination were prepared by ion exchange as described previously [28]. The IR spectra were recorded using a special portable vacuum cell [29]. A steel rod with a wafer holder at one end was used to transfer the samples from the pretreatment region to the end which contains the infrared transmitting (NaCl) windows for spectral measurements. The cell was attached to a high vacuum line capable of producing a final pressure of $< 1.3 \times 10^{-3}$ Nm^{-2}. The zeolite samples, in the form of self supporting discs of surface area 1.3 cm^2, were activated in the IR cell under a stream of nitrogen or hydrogen (120 cm^3 min^{-1}) at 723 K for 18 hours. The discs were then outgassed (at 1.3×10^{-3} Nm^{-2}) at 723 K for a further hour. The sample was kept under vacuum and allowed to cool to room temperature. The cell was then clamped into position in the IR spectrophotometer (Perkin Elmer Model 983G) and the spectrum recorded at room temperature.

All the catalytic reactions were carried out at atmospheric pressure in a fixed bed tubular glass reactor. The details of the catalytic apparatus and test procedure are given elsewhere [29,30]. The W/F value (42.4 g mol^{-1} hr) quoted for cumene cracking represents the mass of hydrated catalyst in grams divided by the feed rate of reactants in moles per hour. Chromatographic analyses were carried out on the liquid samples, collected in a liquid nitrogen trap, using a 5% Bentone/5% di-iso-decylphthalate on Chromosorb W chromatography column with a carrier gas (N_2) flow rate of 30 cm^3 min^{-1} and column temperature at 348 K. The hydrocarbons (BDH) Chemicals Ltd.) used in these studies were of a AnalaR grade and were further dried by standard methods [31].

3. Results and discussion

The chemical composition of the ion exchanged samples have already been tabulated [28]. Sample crystallinity, monitored by X-ray diffraction and IR spectroscopy [32], was maintained for each sample.

3.1. INFRARED STUDIES

Bronsted acidity in zeolites is in the form of structural hydroxyl groups. From a consideration of the reported infrared data [33–36], these surface hydroxyl groups generate two infrared bands: the high frequency (HF) band vibrating in the range 3650–3630 cm^{-1} due to the association of O_1 lattice oxygens with protons in supercage positions generating OH groups which project into the large cavities and are readily accessible to adsorbed molecules; the low frequency (LF) band vibrating in the range 3550–3530 cm^{-1} associated with protons located on O_2, O_3 and O_4 oxygens in the hexagonal prisms and are not easily accessible. These hydroxyl groups exhibit different acid strengths: the cation independent weak acid sites located in the hexagonal prisms (LF band) where the O–H bond is strong; the cation dependent supercage acid sites (HF band) where the O–H

Table 1
Infrared wavenumbers of the residual hydroxyl groups formed on calcining a range of zeolite samples at 723 K

Zeolite sample	Wavenumber/cm^{-1}
LiY	3636
NaY	3648
KY	3686
RbNaY	3695
CsNaY	3710
CuNaY-86.69	3640
CuKY-92.03	3643

bond is relatively weak. On calcination at 723 K, Y zeolites saturated with alkali metal cations and, to a greater extent, exchanged with Cu^{2+} ions slightly dissociate water to generate ill-defined infrared bands in the hydroxyl stretching region. The IR wavenumbers of the hydroxyls thus formed increase with the ionization potential (or electrostatic field) of the exchangeable cation, table 1.

The IR spectrum, in the hydroxyl stretching region of an activated HY zeolite is presented in fig. 1. The spectrum is characterized by two bands at 3640 and 3540 cm^{-1} of similar intensity which is attained on calcining at 673 K and remains constant up to 723 K. The asymmetry of the LF band suggests that the protons of the hexagonal prism are distributed on the three framework oxygens.

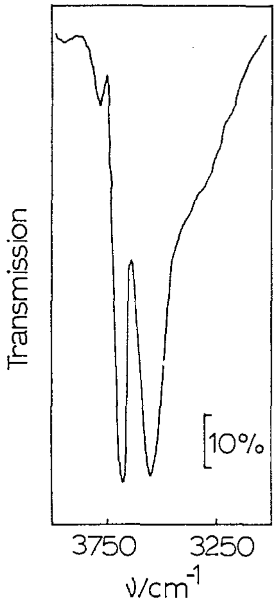

Fig. 1. Infrared spectrum of NH_4Y activated at 723 K.

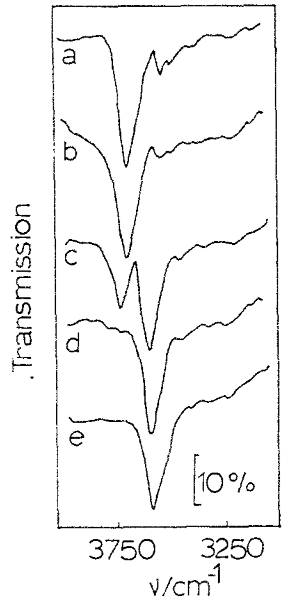

Fig. 2. Infrared spectra of (a) CuLiY-26.34, (b) CuNaY-22.62, (c) CuKY-24.55, (d) CuRbNaY-22.76 and (e) CuCsNaY-19.17 reduced at 723 K.

As has been reported in the literature [36], a third small band due to non-acidic hydroxyls arises at 3740 cm^{-1}.

Heating the copper exchanged zeolites in flowing hydrogen at 723 K generated two highly resolved infrared bands in the hydroxyl stretching region, figs. 2 and 3. In the case of the CuNaY samples, on reduction of the lower loaded samples ($<$ 6 Cu^{2+}), only the HF band arises in the spectrum, fig. 2, indicative of protons being located only in supercage positions. The LF band becomes apparent for exchange levels greater than ca. 6 Cu^{2+}/U.C. (fig. 3) and increases in intensity with further Cu^{2+} exchange. One can therefore postulate that reduction of the CuNaY samples generates supercage hydroxyl groups preferentially; small cage Bronsted acidity is only introduced with the reduction of the more concentrated copper samples. The situation is quite different for the CuKY system, figs. 2 and 3, where one may observe a simultaneous continual increase in the intensities of the HF and LF bands with increasing Cu^{2+} exchange. The potassium system also diverges from the sodium case in that the protons exhibit a preference for the small cage sites; this behavior is more marked at lower copper loadings. The CuLiY samples behave in a similar manner to the sodium system in that the protons show a definite preference for the supercage sites and only begin to locate in the small cages at very high levels of Cu^{2+} exchange. In complete contrast, the protons generated on reduction of CuRbNaY and CuCsNaY locate first in the small cages and only take up positions in the large cages when the former sites have been saturated. The inverse relative intensities generated on the

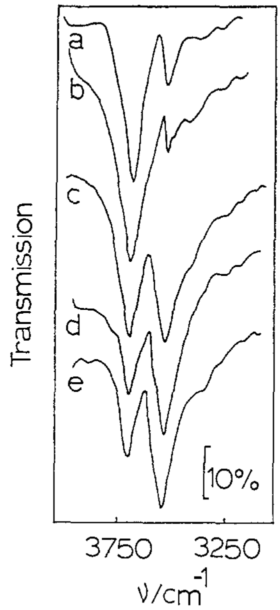

Fig. 3. Infrared spectra of (a) CuLiY-60.79, (b) CuNaY-64.00, (c) CuKY-68.59, (d) CuRbNaY-57.34 and (e) CuCsNaY-57.34 reduced at 723 K.

reduction of CuRbNaY and CuCsNaY compared with that for CuNaY and CuLiY and the intermediate case exhibited by CuKY illustrate the positional effect of the alkali co-cation on the location of the protons and in turn on the location of the potentially active Bronsted acid sites. Arising from this study, the preferential location of protons in the small cages follows the order CuCsNaY > CuRbNaY > CuKY > CuNaY > CuLiY at lower copper loadings. The larger the alkali metal co-cation the greater the tendency for the protons to locate at inaccessible sites. The well shielded small cage protons exhibit lower acid strengths with the result that the greater the tendency for protons to locate in the large cages the greater the enhancement of zeolite acidity yielding the following sequence of increasing acid strength: CuCsNaY < CuRbNaY < CuKY < CuNaY < CuLiY. As the alkali metal cations are progressively exchanged by the divalent copper ions this directional influence is diminished. The observed relative intensities of the HF and LF bands are identical to those exhibited by the nickel exchanged zeolites [37] indicating that the alkali metal co-cations alone influence the location of the generated protons. The different locations preferred by the Cu^{2+} [28] and Ni^{2+} [38] cations in the anhydrous framework therefore have no effect in directing the siting of the protons.

Infrared studies also revealed that the wavenumber of the OH groups is very specific to each alkali metal co-cation. It is well recognized that both HF and LF hydroxyls exhibit characteristic frequencies determined by the charge density of the framework. The shifts to lower frequencies observed within this characteristic

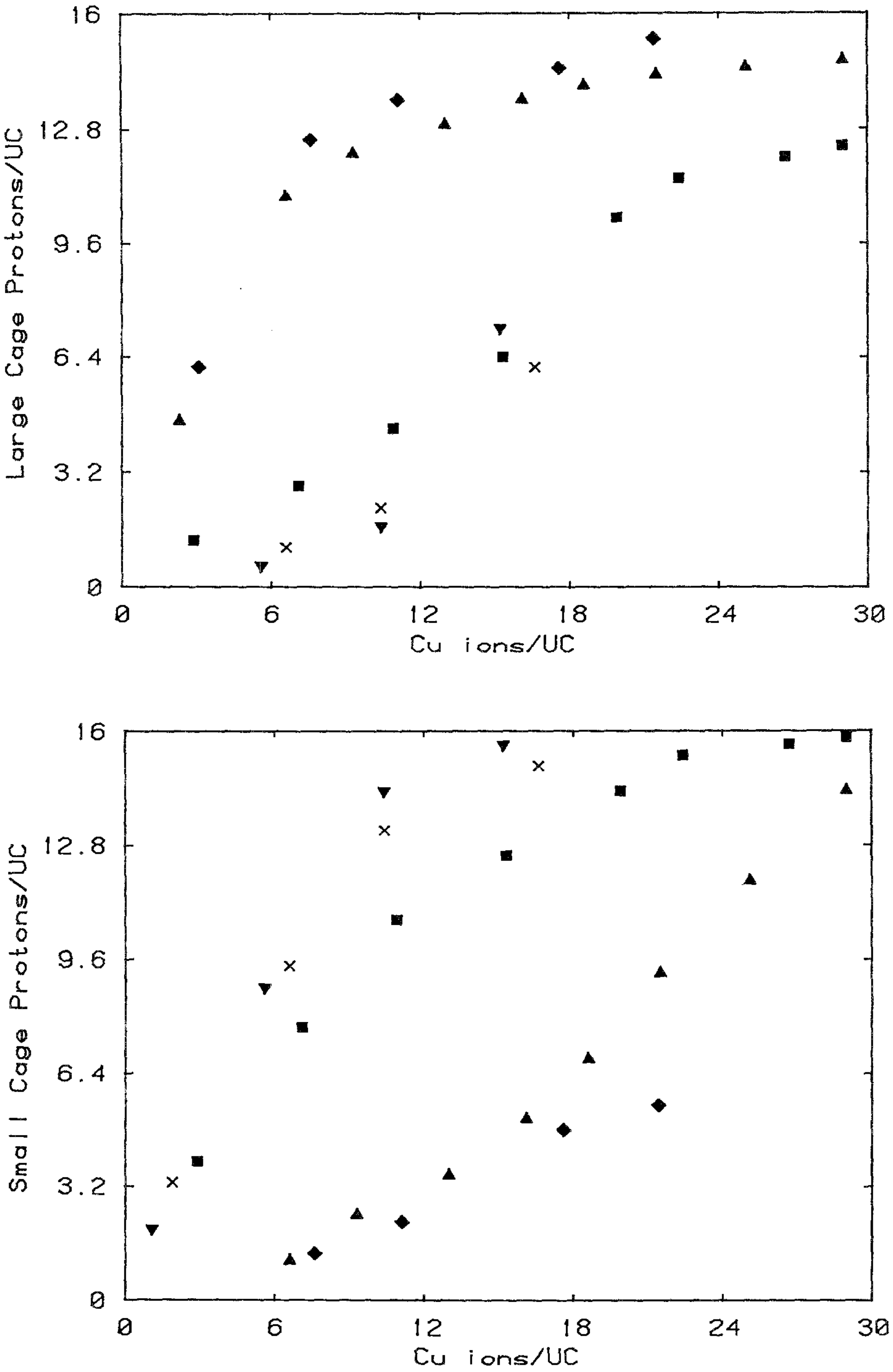

Fig. 4. Plot of the number of (a) large cage and (b) small cage protons generated on the reduction of CuNaY (▲), CuKY (■), CuLiY (◆), CuRbNaY (×) and CuCsNaY (▼) at 723 K as a function of copper loading.

range are related to an increase in polarization and length of the O–H bond which must contribute in consequence to an increase in the hydroxyl acid strength. Table 3 shows the changes in OH wavenumber for a range of reduced copper zeolites at constant metal loading (ca. 7 Cu^{2+}/U.C.). For each sample the shifts observed are greater than the accuracy of measurement. Although the variation of HF and LF wavenumbers is negligible in the copper saturated samples, at alkali metal ion contents greater than ca. 40 ions/U.C. the wavenumbers are markedly cation dependent which reflects a strong influence on the force constant. However, different modifications are observed for the HF and LF bands. The HF wavenumbers are shifted to higher frequencies with increasing bare alkali metal cation size whereas the LF bands exhibit an increase in wavenumber in going from CuLiY to CuKY. However, the CuRbNaY and CuCsNaY samples have LF wavenumbers similar to that for the CuNaY system. The observed independence of the LF band frequency on the Rb^+ and Cs^+ content must be related to the inaccessibility of the sodalite cage to these large cations. Indeed, the better shielded LF hydroxyls exhibit a much smaller dependency of wavenumber on the nature of the counter ion. The rank of acid strength deduced from the order of HF wavenumbers at high alkali contents is CuLiY > CuNaY > CuKY > CuRbNaY > CuCsNaY. This is identical to the order inferred from considerations of proton location. Nevertheless, the data presented in

Table 2
Comparison of the degree of Cu^{2+} reduction values obtained from iodometric titration data with those deduced from the infrared data

Zeolite sample	% Cu^{2+} reduction	
	Iodometric titration	Infrared spectroscopy
CuNaY-8.00	88.86	86.10
CuNaY-34.03	65.36	70.11
CuNaY-55.55	42.36	51.30
CuNaY-86.69	36.14	44.36
CuKY-9.97	76.34	73.14
CuKY-37.45	51.20	58.14
CuKY-52.90	45.13	50.36
CuKY-92.03	39.33	44.40
CuLiY-10.83	87.14	96.20
CuLiY-38.24	48.34	61.14
CuLiY-60.79	34.10	50.00
CuLiY-73.83	27.00	40.30
CuRbNaY-6.41	72.36	69.36
CuRbNaY-35.72	61.69	67.20
CuRbNaY-57.34	54.00	59.33
CuCsNaY-3.93	68.86	67.00
CuCsNaY-35.86	62.00	63.38
CuCsNaY-52.48	60.14	62.11

Table 3
Observed HF and LF wavenumbers of a range of activated zeolites

Zeolite sample	HF band/cm^{-1}	LF band/cm^{-1}
NH_4Y	3640	3540
NiLiY-21.21	3642	3553
NiNaY-22.76	3648	3554
NiKY-23.52	3655	3560
NiRbNaY-18.62	3659	3555
NiCsNaY-22.03	3665	3554
CuLiY-26.34	3640	3550
CuNaY-22.62	3645	3552
CuKY-24.55	3649	3556
CuRbNaY-22.76	3653	3553
CuCsNaY-19.17	3658	3554

table 3 show that the range of reduced metal zeolites exhibit a lower level of acidity compared with the completely decationized HY form.

Assuming that the intensities of the HF and LF bands in fig. 1 are due to 58 H^+/U.C. generated on the calcination of $(NH_4)_{58}Y$, the number of protons generated per unit cell during the reduction of the copper exchanged zeolites was calculated and is illustrated graphically in fig. 4. In addition, assuming that the reduction of each Cu^{2+} cation generates 2 H^+/U.C., the degree of Cu^{2+} reduction was computed from the observed hydroxyl band intensities and are compared with the values obtained from iodometric titrations [28] in table 2. Agreement proved to be quite satisfactory although the values of % Cu^{2+} reduction calculated from the infrared data are greater for most of the samples considered. This results from the presence of additional Bronsted acidity generated during ion exchange and from hydrolysis of water during heat treatment. In addition, the agreement between those two independent methods of measurement is not as good as that observed for the nickel exchanged zeolites [37]. This must be due to the introduction of a higher level of acidity resulting from the stronger electrostatic field associated with the bare Cu^{2+} ion. The stronger polarizing power of the Cu^{2+} cations is reflected in the lower HF and LF wavenumbers compared with those for the nickel zeolites, table 3.

3.2. CATALYTIC STUDIES

(i) Ethylation of benzene

For comparative purposes, it was decided to examine the catalytic activity under conditions where the maximum number of active sites are present. To this end, NH_4Y was heated in a stream of dry nitrogen gas to 723 K. Parent and copper exchanged zeolites were similarly activated. In each cases the benzene : ethanol molar ratio was 3 : 1, nitrogen was used as carrier gas and the

Table 4
Ethylation activity (after 6 hours on stream) of a range of activated oxidized zeolite samples: $C_6H_6:EtOH = 3:1$; $T = 573$ K

Zeolite sample	Mole % ethylbenzene
HY	21.40
LiY	2.10
NaY	1.65
KY	1.20
RbNaY	0.86
CsNaY	0.24
CuNaY-34.03	3.33
CuNaY-64.00	4.85
CuKY-24.55	2.70
CuKY-68.59	4.60

reaction was monitored at half hourly periods. The activated alkali metal and copper exchanged zeolites exhibited a minor degree of ethylation activity which was much lower than that associated with the highly acidic HY catalyst, table 4. Indeed, the rank of catalytic activity, i.e. CsNaY < RbNaY < KY < NaY < LiY < CuY < HY, is consistent with the order of acid strength deduced from infrared and Hammett indicator studies [29,37]. The acidity and hence the activity of these catalysts is therefore determined by the magnitude of the zeolitic electrostatic field.

Reduction of the copper exchanged zeolites generated additional acitivity. % conversion to ethylbenzene as a function of copper loading is presented in fig. 5. It may be noted that activity increases smoothly with copper content for the CuLiY and CuNaY samples whereas in the case of the CuKY samples and more markedly the CuRbNaY and CuCsNaY samples benzene conversions only become apparent at higher copper loadings and then increase smoothly with further exchange. In short, the variation in activity closely mirrors the observed siting of protons in the accessible supercages. The order of increasing activities, i.e. CuCsNaY < CuRbNaY < CuKY < CuNaY < CuLiY, can therefore be attributed to the fact that the more polarizing the co-cation, the easier it is for the OH group to be polarized thus increasing the overall acidity of the Bronsted sites. Thus, acid catalytic activity is essentially associated with Bronsted centers located in the accessible large cages. As expected, the copper exchanged zeolites exhibit a higher level of activity compared with the nickel system [29]. In fact, the higher copper-loaded samples show higher levels of ethylbenzene formation compared to HY (i.e. 16.4%) after six hours on stream. The HY support exhibited a continuous slow deactivation due to catalyst aging as a result of coke deposition whereas the activity exhibited by the copper zeolites remained constant after ca. 5 hours on stream. The presence of copper species on the support must serve to prolong the lifetime of the catalyst by inhibiting of coke formation.

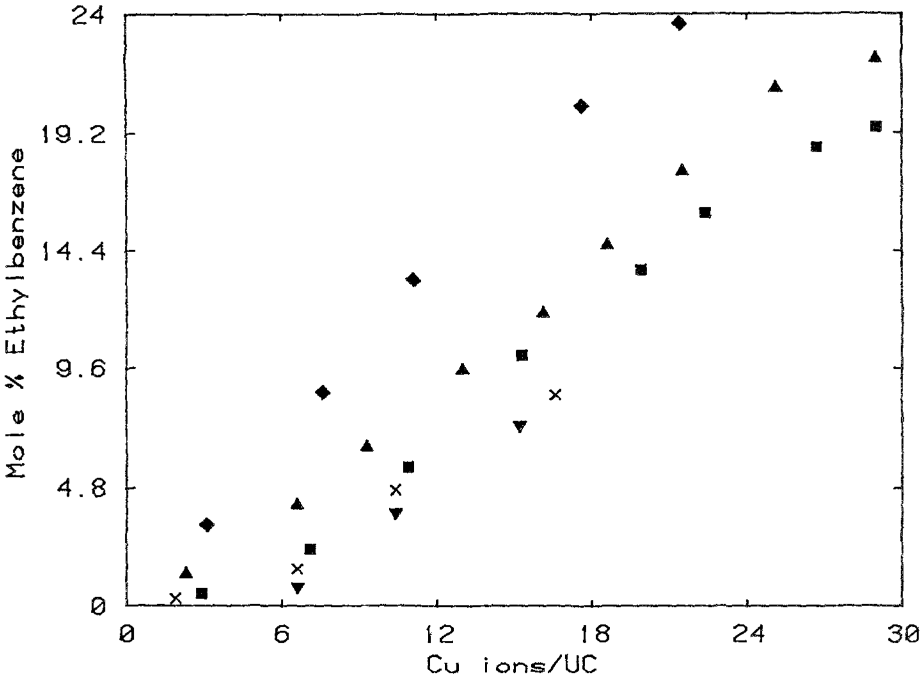

Fig. 5. Variation of benzene ethylation (after 6 hours on stream) over CuNaY (▲), CuKY (■), CuLiY (◆), CuRbNaY (×) and CuCsNaY (▼) with copper loading: C_6H_6: EtOH = 5 : 1; $T = 573$ K.

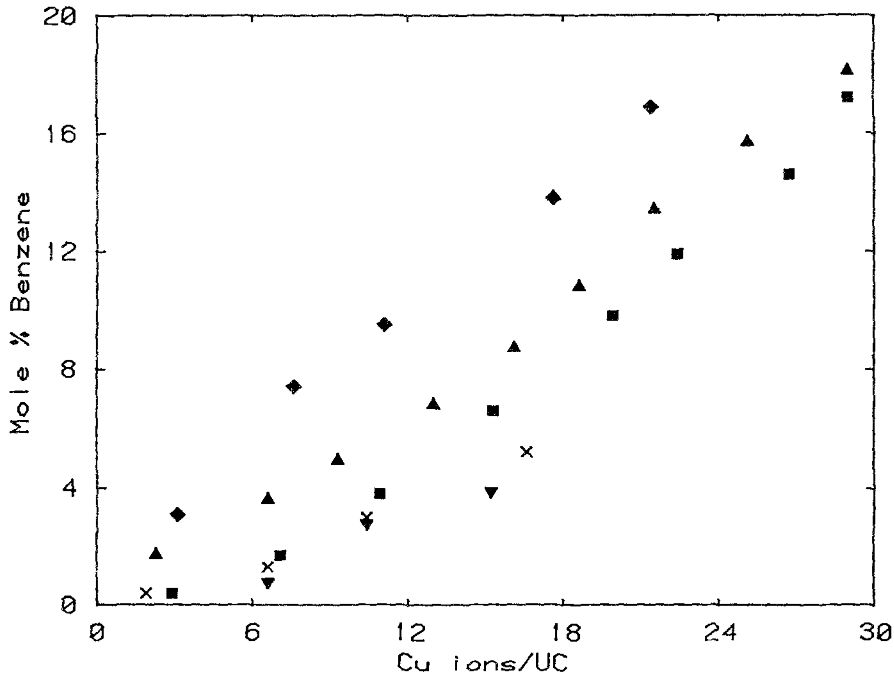

Fig. 6. Variation of cumene cracking (after 6 hours on stream) over CuNaY (▲), CuKY (■), CuLiY (◆), CuRbNaY (×) and CuCsNaY (▼) with copper loading: $W/F = 42.4$ g mol^{-1} hr; $T = 573$ K.

(ii) Cumene cracking

Cumene conversion at the low cumene concentrations studied resulted in the formation of benzene, propylene and coke (which was monitored by carbon microanalysis of the spent catalysts). The dependence of cumene conversion on copper loading, fig. 6, follows the general trends observed for benzene ethylation. However, the actual level of conversion is lower for the cumene reaction which suggests that stronger acid sites are associated with aromatic cracking. In addition, catalysis over the copper rich CuNaY and CuLiY samples yielded higher levels of benzene compared with HY (16.1% C_6H_6 after six hours on stream).

4. Conclusions

From the reported infrared data it is shown that the alkali metal co-cations exhibit specific positional influences on the location of the protons generated on reduction of the supported Cu^{2+} cations; the larger the counter ion, the greater the tendency of the protons to locate in the small cages. The inferred order of increasing acidity, CuCsNaY < CuRbNaY < CuKY < CuNaY < CuLiY, agrees with the observed activities for benzene ethylation and cumene cracking. The presence of copper on the support serves to stabilize the catalytic activity by prolonging the lifetime of the catalyst.

References

[1] P.A. Jacobs, *Carboniogenic Activity of Zeolites* (Elsevier Sci. Publ. Co., Amsterdam, 1977).
[2] J. Hoffmann, B. Hunger, U. Streller, Th. Stock, D. Dombrowski and A. Barth, Zeolites 5 (1985) 31.
[3] J.W. Ward, J. Catal. 22 (1971) 237.
[4] D. Bartomeuf in: *Molecular Sieves II*, ACS Symp. Ser. 40 (1977) 453.
[5] M. Suzuki, K. Tsutsumi and H. Takahashi, Zeolites 2 (1982) 51.
[6] J. Datka, JCS Faraday I, 76 (1980) 705.
[7] K.H. Steinberg, Kh.M. Minachev, H. Bremer, R.V. Dmitriev and A.N. Detyuk, Z. Chem. 15 (1975) 372.
[8] D. Barthomeuf, J. Phys. Chem. 83 (1979) 249.
[9] P.B. Venuto, in: *Molecular Sieve Zeolites II*, Adv. Chem. Ser. 102 (1971) 260.
[10] B. Coughlan, W.M. Carroll and J. Nunan, JCS Faraday I, 79 (1983) 281.
[11] P.N. Mukheryer and P.K. Basu, Chem. Age. India 33 (1982) 202.
[12] J.W. Ward, J. Catal. 11 (1968) 251.
[13] B.V. Liengme and K.W. Hall, Trans. Faraday Soc. 62 (1966) 3229.
[14] B.E. Pickert, A.B. Bolton and M.A. Lanewala, Chem. Eng. Progr. Symp. Ser. 63 (1967) 50.
[15] K.A. Becker, H.G. Karge and W.D. Streubel, J. Catal. 28 (1973) 403.
[16] T. Yashima, H. Ahmod, K. Yamazaki, M. Katsuata and N. Hara, J. Catal. 16 (1970) 273.
[17] A. Abohulguma, Ph.D. Thesis, National University of Ireland (1984).
[18] J.G. Nunan, Ph.D. Thesis, National University of Ireland (1981).
[19] C.S. Huang and A.N. Ko, Tunghai Journal 27 (1986) 679.

[20] P.B. Venuto and P.S. Landis, Adv. Chem. 18 (1968) 259.

[21] J.T. Richardson, J. Catal. 9 (1967) 182.

[22] W.J. Hatcher Jnr., Ind. Eng. Prod. Res. Dev. 24 (1985) 10.

[23] D.A. Best and B.W. Wojciechowski, J. Catal. 47 (1977) 343.

[24] J.A. Rabo and M.L. Poutsma, in: *Molecular Sieve Zeolites II*, ACS Symp. Ser. 42 (1978) 284.

[25] K. Tsutsumi, S. Fuji and H. Takahashi, J. Catal. 24 (1972) 8.

[26] S. Beran, J. Phys. Chem. 89 (1985) 5586.

[27] E. O'Donoghue and D. Barthomeuf, Zeolites 6 (1986) 267.

[28] M.A. Keane and B. Coughlan, JCS Faraday I (1990), Manuscript 9/03620B accepted for publication.

[29] M.A. Keane, A catalytic and characterization study of the effects of alkali metal cations on nickel and other transitions metals in Y zeolite catalysts. Ph.D. Thesis (Volumes 1 and 2), National University of Ireland, 1988.

[30] M.A. Keane and B. Coughlan, Zeolites (1990) submitted for publication.

[31] Vogel, *Practical Organic Chemistry* (Longmans, London & New York Publ., 1978).

[32] E.M. Flanigen, H. Khatami and H.A. Szymauski, in: *Molecular Sieve Zeolites*, Adv. Chem. Ser. 101 (1971) 201.

[33] V.B. Kazansky, in: *Structure and Reactivity of Modified Zeolites*, Stud. Surf. Sci. Catal. 18 (1984) 61.

[34] J.M. Thomas and C. Williams, in: *Chemical Reactions in Organic and Inorganic Constrained Systems*, ed. R. Setton (D. Reidel Publ. Co., 1986) p. 49.

[35] A. Bielanski and J. Datka, J. Catal. 37 (1975) 383.

[36] D.H. Olson and E. Dempsey, J. Catal. 13 (1969) 221.

[37] M.A. Keane and B. Coughlan, J. Colloid. Interf. Sci. (1990), Manuscript 8161K accepted for publication.

[38] M.A. Keane and B. Coughlan, J. Catal. (1990), Manuscript H0423 accepted for publication.